Potential Energy Surfaces for the Reaction of O Atoms with CH_3I: Implications for Thermochemistry and Kinetics

Ashutosh Misra,[†,§] R. J. Berry,[‡] and Paul Marshall*[,†,‡]

Department of Chemistry, University of North Texas, PO Box 305070, Denton, Texas 76203, and Center for Computational Modeling of Nonstructural Materials, Wright Laboratory, Wright-Patterson Air Force Base, Ohio 45433

Received: April 17, 1997; In Final Form: July 10, 1997[⊗]

The geometries of IO, HClO, ICH_2O, CH_3IO, CH_3OI, CH_2IOH, and ICH_2OH have been obtained at the HF and MP2(FU)/6-31G(d) levels of ab initio theory, and the HF/6-31G(d) frequencies are compared with experimental assignments where these are available. The Gaussian-2 method was used to provide thermochemical data for use in atmospheric and combustion modeling. Transition states that connect these species have also been characterized, and the results were used to develop the singlet and triplet potential energy surfaces for the reaction $O(^3P) + CH_3I$. These surfaces explain the complex behavior of this reaction, and a QRRK analysis over 200−2000 K gave good accord with recent kinetic and product studies by Gilles et al. [*J. Phys. Chem.* **1996**, *100*, 14005]. IO is predicted to be the dominant product below about 2000 K. Other likely products are OH and the collisionally stabilized adducts CH_3IO and ICH_2OH, and the latter's fragmentation products that include H and HI.

Introduction

The consideration of iodofluorocarbons as possible substitutes for halons such as CF_3Br in some fire suppression applications[1] requires knowledge of the combustion chemistry of iodine compounds. Much of the necessary kinetic and thermochemical information is unavailable experimentally, and one goal of the present work is to address this deficiency via ab initio methods. Here we present singlet and triplet potential energy surfaces for the $C/H_3/I/O$ system, where bound minima and transition states are characterized at the Gaussian-2 (G2) level of theory. The results yield the thermochemistry of several iodine-containing species that may play roles in flame suppression by iodofluorocarbons, and the potential energy surfaces are employed to analyze the kinetics and product channels for the reaction of atomic oxygen with iodomethane:

$$CH_3I + O(^3P) \rightarrow \text{products} \qquad (1)$$

As revealed by the detailed experiments of Ravishankara and co-workers,[2] reaction 1 exhibits complex behavior, which includes the formation of multiple products (IO, OH, H, and HI) and a total rate constant k_1 which is much greater than that for the reactions of the fluoro, chloro, and bromo analogues. The known products account for only about 70% of reaction 1. One aim of the present work is to help identify the other products. This reaction is also of potential importance in the atmospheric chemistry of CH_3I, which has recently been proposed as a contributor to ozone destruction in the lower stratosphere.[3]

The analysis yields the first thermochemical information about several oxygenated carbon−iodine species, which is central to the development of plausible mechanisms for both atmospheric and combustion systems. The molecules characterized include formyl iodide (CHIO), the major photooxidation product of CHI_3,[4] and the species detected following irradiation of CH_3I/O_3 mixtures in a frozen matrix: iodosomethane (CH_3IO), methyl hypoiodite (CH_3OI), and iodomethanol (ICH_2OH).[5] Some species have not yet been detected to date, including iodomethoxy (ICH_2O) and the novel CH_2IOH, which has no counterpart in the chemistry of lighter halomethanes. Computed vibrational frequencies fill gaps in the partial IR spectra.

Ab Initio Methodology

The extension of Pople and co-workers' G2 method[6] to iodine compounds by Glukhovstev et al.[7] has been described in detail elsewhere. In brief, the geometry of each stationary point on the potential energy surface (PES) was initially optimized at the HF/6-31G(d) level of theory, and vibrational frequencies were obtained and scaled by a standard factor of 0.8929. These frequencies are needed to calculate the zero-point vibrational energy and thermodynamic properties, and the number of imaginary frequencies, 0 or 1, confirmed whether a bound minimum or a transition state (TS) had been located. The geometry was then reoptimized at the MP2(FU)/6-31G(d) level of theory, which includes a partial correction for the effects of electron correlation. MP2 frequencies were recomputed as a check but, unless noted, were not employed in the subsequent analysis. Next, a series of higher-level calculations were performed, which were combined to yield the G2 or approximate QCISD(T)/6-311+G(3df,2p) energy. The computations were carried out with the GAUSSIAN94 program[8] on Silicon Graphics Indigo 2 and Power Challenge computers.

This G2 approach is the all-electron (no effective core potential) method which, in limited comparisons, appears to perform at least as accurately as the G2[ECP] method, even though no explicit allowance for relativistic core effects is included.[7] These effects appear to cancel between reactants and products. Spin−orbit coupling is of potential importance, and corrections[7] derived from the experimental spin−orbit splitting are employed for the energies of I and IO at 0 K.

† University of North Texas.
‡ Wright-Patterson Air Force Base.
* To whom correspondence should be addressed.
§ Present address: Air Liquide Electronics Chemicals and Services, Inc., 13546 North Central Expressway, MS 301, Dallas, TX 75243.
⊗ Abstract published in *Advance ACS Abstracts,* September 1, 1997.

S1089-5639(97)01337-6 CCC: $14.00

TABLE 1: Gaussian-2 Energies and Derived Enthalpies of Formation

species	E_0(G2), au[a]	$\Delta_f H_0$, kJ mol^{-1}	$\Delta_f H_{298}$, kJ mol^{-1}
HClO	−7030.775 78	−61.0	−64.9
ICH_2O	−7031.293 36	93.9	85.7
CH_3IO	−7031.870 36	108.9	99.3
CH_3OI	−7031.926 99	−35.5	−46.9
CH_2IOH	−7031.860 04	136.0	121.9
ICH_2OH	−7031.962 16	−121.0	−133.7
IO	−6992.061 22[b]	128.4	126.5
		(113.6)[c]	(111.7 ± 3.8)[c]
TS1	−7031.796 09	311.7	301.7
TS2	−7031.807 77	275.4	264.4
TS3	−7031.820 74	239.7	228.5
TS4	−7031.833 16	212.1	201.3
TS5	−114.819 95	160.3	153.4
TS6	−7031.907 98	24.1	11.8
TS7	−7031.833 88	210.7	199.7
TS8	−7031.822 17	250.2	238.1

[a] 1 au ≈ 2625.5 kJ mol^{-1}. [b] Using the experimental ZPE and −0.005 31 au spin−orbit correction. [c] Experimental value from ref 16.

Results and Discussion

Iodine Monoxide. IO is the major product of reaction 1.[2] The computed bond length is 1.992 and 1.939 × 10^{-10} m at the HF and MP2(FU)/6-31G(d) levels of theory, respectively. The latter value, employed in the G2 calculations below, agrees only moderately well with the experimental value of 1.868 × 10^{-10} m.[9] The scaled computed frequency at these two levels is 432 and 707 cm^{-1}, respectively, showing that the HF value is in poor agreement with the experimental ν_0 of 673 cm^{-1}.[9] Inclusion of electron correlation has improved the agreement with experiment, and higher-level QCISD(T)/6-311+G(3df) computations recently performed by McGrath and Rowland[10] led to even better accord. For the purposes of computing ZPE and thermal energy corrections to the G2 energy (see Table 1), we employ the experimental frequency, geometry, and spin−orbit splitting.[9]

Huie and Laszlo have recently reviewed the thermochemistry of IO and noted that estimates of the heat of formation are very widely scattered and range from 107 to 175 kJ mol^{-1}.[11] They recommended a value of 130 kJ mol^{-1}, based on the average of two molecular beam studies[12,13] which they considered to be the most reliable experiments. Here we estimate $\Delta_f H$(IO) via a series of working reactions that relate the thermochemistry of IO to that of other small iodine-containing species, by calculation of the 0 K enthalpy change, $\Delta_r H_0$, for each reaction combined with the known $\Delta_f H_0$ of all species except IO. For HOI we employ our experimentally based $\Delta_f H_0$ of −65 ± 7 kJ mol^{-1}.[14] The reactions and results are summarized in Table 2, and the mean $\Delta_f H_0$(IO) is 128 ± 11 kJ mol^{-1} (±2σ). This result implies $\Delta_f H_{298}$(IO) = 126.5 ± 11 kJ mol^{-1}, which is in good accord with the recommendation of Huie and Laszlo and an earlier recommendation of 130 ± 13 kJ mol^{-1} by Gurvich et al.[9] McGrath and Rowland recently employed higher-level G2(QCI) theory and the two working reactions

$$Cl + IO \rightarrow ClO + I$$

$$Br + IO \rightarrow BrO + I$$

to derive $\Delta_f H_0$ and $\Delta_f H_{298}$ values of 129.7 ± 4.2 and 127.8 kJ mol^{-1}, respectively.[10] Hassanzadeh and Irikura very recently computed the thermochemistry of IO^-, which together with the experimental electron affinity of IO yielded $\Delta_f H_{298}$(IO) = 118.8 ± 7.6 kJ mol^{-1}.[15] Analysis of the temperature dependence of

$$CH_3I + O(^3P) \rightarrow CH_3 + IO \qquad (2)$$

TABLE 2: Heat of Formation of IO

working reaction	derived $\Delta_f H_0$/kJ mol^{-1}
$IO \rightarrow I + O$	138.8
$IO + {}^3/_2\ H_2 \rightarrow HI + H_2O$	129.0
$I + ClO \rightarrow IO + Cl$	128.0
$IO + H_2O \rightarrow HOI + OH$	126.8
$IO + HOCl \rightarrow HOI + ClO$	118.0
$IO + ClCN \rightarrow ICN + ClO$	129.0
$IO + HNO \rightarrow INO + OH$	129.1
mean ± 2σ	128.4 ± 11.2

led Gilles et al. to conclude that reaction 2 is not endothermic and that therefore $\Delta_f H_{298}$(IO) ≤ 120.5 kJ mol^{-1}.[2] This result is in accord with the kinetic measurements of Bedjanian et al.,[16] who bracketed the thermochemistry via the activation energies of $I + OClO \rightarrow IO + ClO$ and $Cl + IO \rightarrow I + ClO$ and obtained $\Delta_f H_{298}$(IO) = 111.7 ± 3.8 kJ mol^{-1}. This measurement lies significantly below most of the computed values (except that from Hassanzadeh and Irikura[15]) and shows that the IO bond strength is difficult to compute accurately. The G2 range for $\Delta_f H_{298}$(IO) given above just reaches the experimental range; because the measurement has a small uncertainty and should be accurate, it is employed in the kinetic analysis below.

Oxygenated Species. The MP2(FU)/6-31G(d) geometries of HClO, ICH_2O, CH_3IO, CH_3OI, CH_2IOH, and ICH_2OH are illustrated in Figure 1. Vibrational frequencies at the HF/6-31G(d) level, scaled by the standard factor of 0.8929, are summarized in Table 3. None of these geometries have been measured but there is overall good agreement with the experimental vibrational frequencies.[4,5] One conspicuously poor comparison is for CH_3IO where, as in the case of IO discussed above, the I−O stretching frequency is underestimated at the HF/6-31G(d) level of theory. The error of 187 cm^{-1} does however contribute only 1.1 kJ mol^{-1} to the ZPE. In general, any errors in high-frequency C−H and O−H stretching modes largely cancel in our thermochemical analysis.

The enthalpies of formation of the oxygenated species are obtained via the G2 $\Delta_r H_0$ values for a set of working reactions:

$$HClO + CH_4 \rightarrow CH_2O + CH_3I$$

$$ICH_2O + CH_4 \rightarrow CH_3O + CH_3I$$

$$CH_3IO + HI \rightarrow CH_3I + HOI$$

$$CH_3OI + H_2O \rightarrow CH_3OH + HOI$$

$$CH_2IOH + HI \rightarrow HOI + CH_3I$$

$$ICH_2OH + CH_4 \rightarrow CH_3OH + CH_3I$$

Because $\Delta_f H_0$ is known for each participant except the first in each reaction, the unknown $\Delta_f H_0$ is then derived from the computed $\Delta_r H_0$. The $\Delta_f H_0$ values for the C/H/O species were taken from the evaluation of Gurvich et al.[9] An exception is CH_2OH, for which we employed a more recent value obtained by Seetula and Gutman.[17] These reactions, by contrast to the usual atomization step employed in a G2 analysis, conserve the number and type of each bond between heavy atoms, and therefore residual errors in the G2 energies arising from basis set incompleteness and inadequate correlation treatment largely cancel. In particular, these reactions conserve any I−O bonds, whose strengths, as noted in the previous section, are hard to compute accurately. The corresponding $\Delta_f H_{298}$ values are obtained via experimental $H_{298} - H_0$ values for the elements in their reference states[18] and ancillary molecules[9] together with ab initio values for the unknown iodine-containing species. The

TABLE 3: Comparison of Experimental and Scaled HF/6-31G(d) Vibrational Frequencies (cm^{-1})

HCIO			ICH_2O			CH_3IO		
mode	expt[a]	calc	mode	expt	calc	mode	expt[c]	calc
OCI bend[b]		299	OCI bend		212	CH_3 rotation		68
CI stretch[b]		558	CI stretch		405	CIO bend		158
out-of-plane		879	CH_2 twist		858	CI stretch	497	503
HCO bend	1248	1271	CO stretch		1027	IO stretch	724	537
CO stretch	1776	1816	HCI bend		1394	CH_3 rock	848	881
CH stretch	2930	2920	CH_2 scissor		1493	CH_3 rock	859	885
			HCO bend		1561	CH_3 umbrella		1285
			CH_3 sym str		2922	CH_3 def	1223	1421
			CH_3 asym str		2992	CH_3 def	1400	1438
						CH_3 sym str	2945	2914
						CH_3 asym str		3015
						CH_3 asym str		3030

CH_3OI			CH_2IOH			ICH_2OH		
mode	expt[c]	calc	mode	expt	calc	mode	expt[c]	calc
CH_3 rotation		203	OIC bend		151	OCI bend		250
COI bend		277	OH rotation		288	OH rotation		397
IO stretch	528	546	CIO asym str		483	CI stretch		492
CO stretch	1074	1038	CH_2 twist		535	CH_2 twist		841
CH_3 rock		1150	CIO sym str		548	CO stretch	999	1094
CH_3 rock		1167	CH_2 wag		822	HOC bend		1138
CH_3 umbrella		1446	CH_2 wag		888	HCI bend		1263
CH_3 def		1462	HOI bend		961	HCO bend		1363
CH_3 def		1479	HCI bend		1389	CH_2 scissor	1466	1476
CH_3 sym str		2865	CH_2 sym str		2981	CH_2 sym str	2815	2956
CH_3 asym str		2928	CH_2 asym str		3089	CH_2 asym str	2937	3054
CH_3 asym str		2947	OH stretch		3647	OH stretch	3350	3660

[a] Reference 4. [b] Strongly mixed modes. [c] Reference 5.

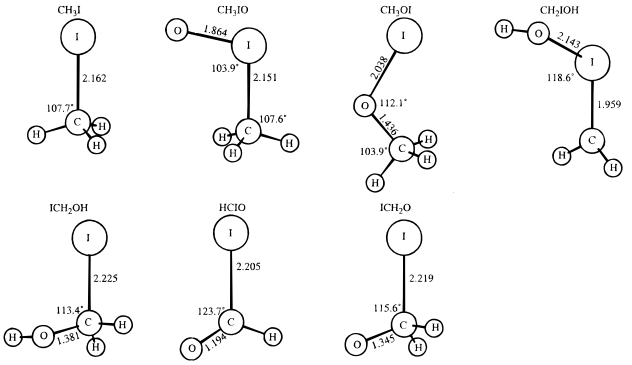

Figure 1. Geometries of bound species in the singlet and triplet PESs for O + CH_3I obtained at the MP2(FU)/6-31G(d) level of theory.

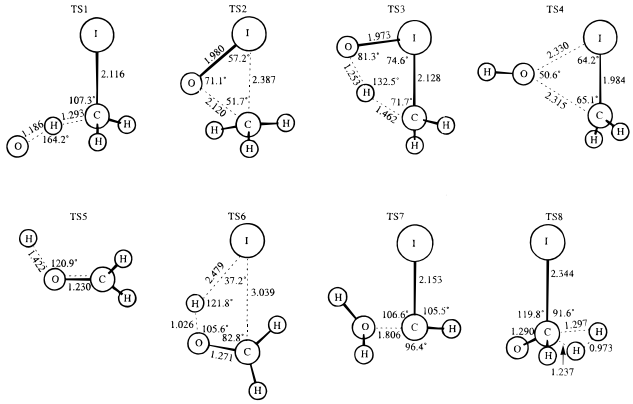

Figure 2. Geometries of transition states in the singlet and triplet PESs for O + CH_3I obtained at the MP2(FU)/6-31G(d) level of theory.

resulting thermochemistry is summarized in Table 1; none of these quantities have apparently been measured before. The quoted uncertainties in the input experimental $\Delta_f H_0$ values range from 0.1 to 7 kJ mol^{-1} [9] and represent a lower bound to the uncertainty of the G2-based thermochemistry. We provisionally suggest error limits of ±10 kJ mol^{-1}, in line with the G2 target accuracy for first- and second-row elements.[6]

Triplet Potential Energy Surface. Singlet and triplet PESs for O + CH_3I are shown in Figure 3. Where available, experimental values of $\Delta_f H$ have been employed; computed values of $\Delta_f H$ were used for the unknown iodine species and the TSs. Grice and co-workers have noted the possibility of intersystem crossing for the ethyl analogue of reaction 1.[19] We find this crossing permits access to a rich chemistry based partly on the ability of iodine to bond divalently and partly on the modest barriers to isomerization/dissociation of various intermediates because of the fairly low O−I and C−I bond strengths. Transition states have been characterized, and the geometries are shown in Figure 2, the energies are summarized in Table 1, and the frequencies are listed in Table 4. The imaginary normal mode of each TS was visualized to help identify the connected reactants and products, and in some cases the reaction coordinate

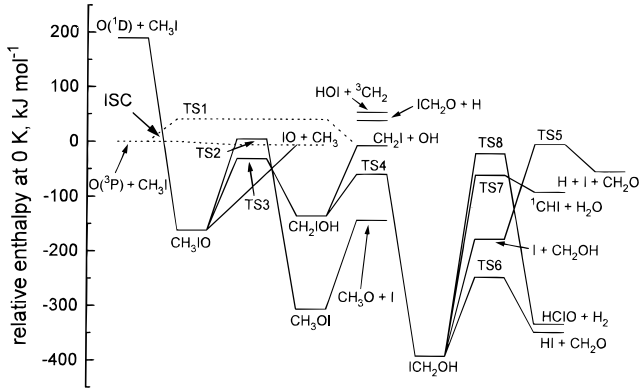

Figure 3. Singlet (solid lines) and triplet (dotted lines) PESs for O + CH_3I, with intersystem crossing (ISC), showing relative enthalpies at 0 K (experimental data used for I, IO, HOI, CH_3I, and C/H/O species, G2-based data for other minima and the transition states).

was followed for confirmation. The $\Delta_f H_0$ for each TS was obtained as the average of the values derived from its G2 energy relative to the reactants and products connected by the TS. The

TABLE 4: Vibrational Frequencies (cm^{-1}) of Transition States

transition state	frequencies[a]
TS1	2787i, 92, 353, 411, 566, 805, 861, 1011, 1090, 1355, 2967, 3064
TS2	773i, 220, 330, 414, 699, 768, 1193, 1392, 1420, 2993, 3145, 3180
TS3	1821i, 214, 353, 509, 667, 805, 1019, 1280, 1379, 1754, 2934, 3015
TS4	404i, 241, 346, 416, 638, 780, 832, 855, 1388, 3027, 3151, 3542
TS5	1546i, 435, 673, 896, 1180, 1286, 1505, 2899, 2997
TS6	515i, 197, 442, 916, 999, 1116, 1357, 1398, 1552, 2717, 3071, 3212[b]
TS7	1713i, 209, 409, 442, 527, 893, 963, 1120, 1367, 2189, 3050, 3626
TS8	2250i, 245, 490, 588, 887, 963, 1189, 1238, 1466, 1978, 2148, 2939

[a] HF/6-31G(d) values scaled by 0.8929. [b] MP2(FU)/6-31G(d) values scaled by 0.95.

difference between the two values is a measure of the internal consistency of the thermochemical analysis: here the mean of the absolute differences is 5.4 ± 7.6 kJ mol^{-1} ($\pm 2\sigma$).

At all levels of theory employed here reaction 2 is computed to be at least slightly endothermic, a deficiency in the calculations, and no barrier beyond this apparent endothermicity was located. The experimental thermochemistry implies that IO formation is exothermic by 6 ± 4 kJ mol^{-1} at 298 K. Thus, IO might be formed by direct abstraction along the triplet PES. However, as argued below, there is probably a contribution from the singlet PES as well.

The computed barrier to direct H abstraction was used to calculate the rate constant for

$$O(^3P) + CH_3I \rightarrow OH + CH_2I \qquad (3)$$

by means of conventional transition-state theory as implemented in the POLYRATE program:[20]

$$k_3 = \Gamma \frac{k_B T}{h} \frac{Q_{TS}}{Q_{reactants}} \exp\left(-\frac{E_0^{\ddagger}}{RT}\right) \qquad (4)$$

A one-dimensional tunneling correction Γ was applied, based on an Eckart potential fitted to the forward and reverse barriers and the imaginary frequency.[21,22] The *Q*s are the partition functions, and $E_0^{\ddagger}$ is the enthalpy of the TS relative to the reactants at 0 K. The k_3 results are shown in Arrhenius form in Figure 4, together with the measured rate constant for OH production (16% yield) of Gilles et al.[2] The computed results differ by a factor of 10^4 from this measurement at room temperature and thereby suggest that another pathway is involved in OH production.

Intersystem Crossing. Intersystem crossing (ISC) from the triplet to the singlet PES, mediated by spin−orbit coupling near the iodine atom, permits the formation of a CH_3IO adduct. We have explored the intersection of the singlet and triplet PESs, and the results are shown in Figure 5. QCISD(T)/6-311G(d,p) energies are plotted as a function of the I−O separation for two trajectories, a collision between O and CH_3I where I−O is collinear with the C−I bond, and a collision where the C−I−O angle is 109° (the same angle as in the CH_3IO adduct). It may be seen that there is a large singlet−triplet energy gap for collinear collisions and that at all I−O separations the triplet remains the ground state, so that ISC is not possible. C−I−O bending stabilizes the singlet state, and for collisions at 109° to the C−I bond ISC is feasible at an I−O distance of about 2.3 × 10^{-10} m with only a modest barrier. This picture is expected

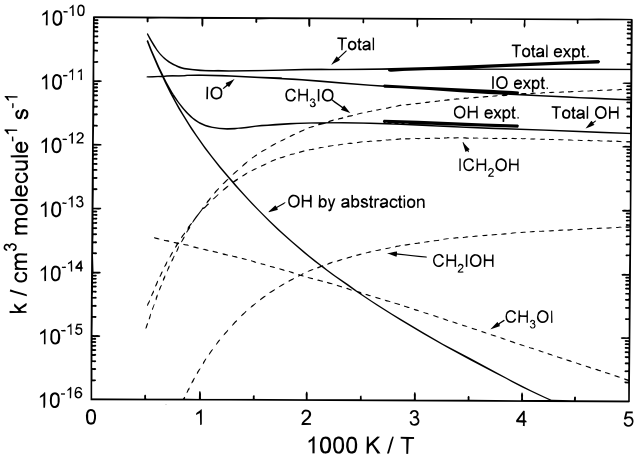

Figure 4. Results of a QRRK analysis of product channels of $O(^3P)$ + CH_3I in 50 Torr of N_2 as a function of temperature. The dashed lines represent adducts. "ICH_2OH" and "CH_3OI" include possible fragmentation products. The heavy lines represent experimental results obtained by Gilles et al.[2]

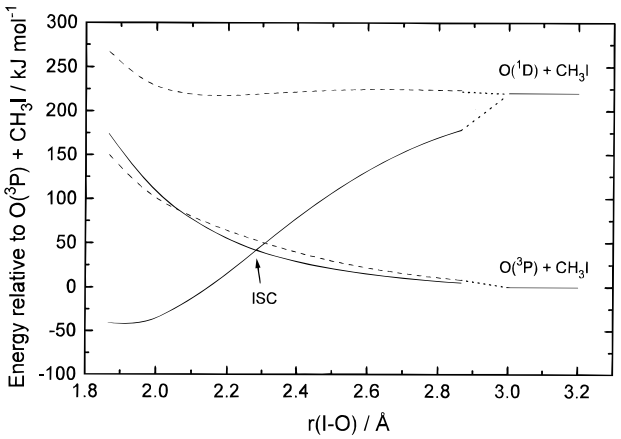

Figure 5. Relative QCISD(T)/6-311G(d,p) energies for singlet and triplet states of O + CH_3I as a function of I−O separation in linear (dashed lines) and bent (solid lines) C−I−O configurations.

to be qualitatively correct, although the level of theory employed for these scans of the PESs is significantly below that used to characterize the various stationary points discussed in section 2.

Singlet Potential Energy Surface. The CH_3IO adduct formed via intersystem crossing will be initially excited by about 160 kJ mol^{-1}, and we have explored several isomerization/dissociation pathways. Because there is no distinct energy barrier to dissociation to CH_3 + IO there will be a loose, entropically favored TS for this process. This pathway, in combination with a possible contribution from direct abstraction on the triplet PES, presumably accounts for IO formation, which is the observed dominant product channel (44% branching ratio at 298 K).[2]

CH_3IO could isomerize via a three-center TS to more stable CH_3OI, but this is the least favorable pathway both entropically and energetically. Consistent with this idea, CH_3O, which would be formed easily by O−I bond fission in initially excited CH_3OI, was *not* observed experimentally (branching ratio < 3%).[2] CH_3IO may also rearrange via a four-center TS to form the novel species CH_2IOH. The singlet spin-restricted RHF wave function of this molecule is unstable with respect to a spin-unrestricted UHF wave function, so the molecule appears to have some diradical character. Simple I−O bond fission in CH_2IOH, expected to proceed through a loose TS and therefore with a large preexponential factor, leads to OH formation and provides a pathway where none of the barriers lie above the

energy of the reactants. This pathway can therefore account qualitatively for the fast observed OH production,[2] unlike direct abstraction on the triplet PES. A tighter but lower energy TS leads from CH_2IOH to the most stable species on the singlet PES, ICH_2OH. This will be formed in an energized state and may therefore fragment, as illustrated in Figure 3, to CH_2O plus either HI or H + I. We note that both H and HI were observed as minor products (branching ratios approximately 7% and 2%, respectively).[2] Thus, our proposed PES is able to account qualitatively for all the observed products of reaction 1; the next section summarizes a more quantitative test.

There are several potential reaction channels that would not have been observable in the apparatuses employed by Gilles et al.[15] One example is the channel leading to $^1CHI + H_2O$ which is energetically accessible. Also shown in Figure 3 are two potential products that would not have been detected, HOI (hypoiodous acid) and ICH_2O. We would expect the latter species to dissociate rapidly to $I + CH_2O$, by analogy with $BrCH_2O$.[23,24] Not only are HOI and ICH_2O significantly endothermic products, but also no connecting pathways have been located. This situation may be contrasted to that for $C_2H_5I + O(^3P)$, where it has been shown experimentally that HOI is a major product,[19,25,26] a result which is in accord with the G2 PES we have computed for that reaction.[26,27]

Kinetic Analysis of IO and OH Production. Quantum RRK theory[28] was employed to investigate part of the singlet PES, in a more detailed consideration of the fate of initally excited CH_3IO^* formed by addition of O to CH_3I. The following scheme was considered:

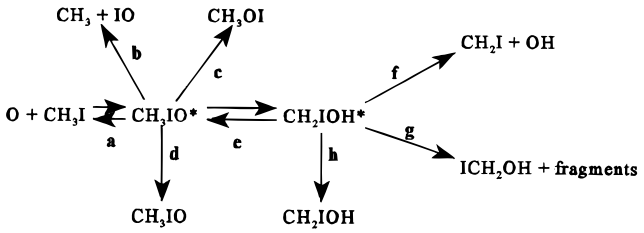

In addition to the energy barriers and vibrational frequencies already calculated, the QRRK analysis requires an assessment of the Arrhenius parameters for the isomerization and dissociation steps at their high-pressure limits. For reactions via clearly defined saddle points in the PES, the preexponential A factors at 298 K for these tight TSs were estimated from the entropy of activation based on the ab initio geometries and frequencies via the relation[29]

$$A = (ek_BT/h)\exp(\Delta S^{\ddagger}/R)$$

For the two simple bond fissions b and f, with no barrier beyond the endothermicity, loose TSs were assumed.[29] The value of A for k_{-a} was based on microscopic reversibility. The adduct formation rate constant k_a was assumed to be equal to the measured total rate constant at 298 K and taken to be temperature independent. For simplicity, steps c and g were treated as irreversible. This is reasonable because CH_3OI and ICH_2OH are more stable than the other intermediate adducts, and if not stabilized by collisions, they will probably fragment rather than undergo reverse isomerization. Enthalpies of activation $\Delta H^{\ddagger}$ were obtained from the ab initio $\Delta_f H_{298}$ values (see Table 1), and yield activation energies E_a for the unimolecular steps at 298 K via the relation[29]

$$E_a = \Delta H^{\ddagger} + RT$$

The stabilization rate constants k_d and k_h were estimated from the standard Lennard-Jones parameters for N_2 bath gas and the average energy transferred per collision,[28] together with a guessed set of Lennard-Jones parameters for the intermediate adducts, which are in line with those for other molecules.[30] The input data for the QRRK calculations are summarized in Table 5.

TABLE 5: Input Parameters for QRRK Model[a]

reaction	A, s^{-1}	E_a, kJ mol^{-1}	reaction	A, s^{-1}	E_a, kJ mol^{-1}
a	1.7×10^{-11} [b]	0	e	2.4×10^{12}	132
−a	3.7×10^{14}	164	−e	5.6×10^{12}	109
b	5×10^{14}	161	f	5.0×10^{16}	140
c	2.9×10^{12}	168	g	8.8×10^{12}	87

[a] Lennard-Jones parameters for CH_3IO and CH_2IOH: $\sigma = 4.3$ Å and $\epsilon/k = 300$ K. Geometric mean frequencies $\bar{\nu}(CH_3IO) = 858$ cm^{-1} and $\bar{\nu}(CH_2IOH) = 875$ cm^{-1}. [b] Units are cm^3 $molecule^{-1}$ s^{-1}.

Three parameters were adjusted to match the experimental rate constants at $T = 298$ K and $p(N_2) = 50$ Torr (1 Torr ≈ 133 Pa):[2] the unknown A factors for paths b and f and the activation energy for path g (which was increased by 5 kJ mol^{-1}). This last adjustment is within the G2 uncertainty, and we further note that the QRRK treatment imposes an energy graining or resolution of $h\bar{\nu}$, where $\bar{\nu}$ is the geometric mean frequency of the adducts, which is about 10 kJ mol^{-1}.

Figure 4 illustrates the good accord between the QRRK results and the measurements of Gilles et al.[2] The QRRK analysis is based on the assumption that all of the reaction proceeds via ISC and that the probability that a collision initially on the triplet PES leads to the singlet PES is high, $\gtrsim 0.1$. Production of IO via the singlet surface is slightly inversely pressure dependent because as the pressure is increased adduct stabilization rather than fragmentation begins to become favored. The QRRK-predicted branching ratio for IO formation drops by a factor of 1.5 upon changing the pressure from from 1 to 50 Torr. Experimentally, the branching ratio was found to be pressure independent, but there was significant uncertainty at the lower end of this pressure range.[2] If a separate channel for IO formation by direct abstraction on the triplet PES was allowed for, which would be pressure independent, then the modeled IO branching ratio would be less sensitive to pressure. Presently, the uncertainties in the computed and measured rate constants do not permit a definitive answer to the relative importance of singlet and triplet production pathways. CH_3OI production is calculated to be unfavorable, as suggested above, and the most likely sinks for O atoms at low temperatures, apart from IO and OH, are CH_3IO, ICH_2OH and the latter's fragmentation products which include H and HI. Our QRRK model reproduces the weak temperature dependences observed for IO and OH production. The good match between experiment and theory shown in Figure 4 supports the G2 PES and kinetic analysis, although the fit at 298 K and 50 Torr of N_2 is probably not unique. The fit also yields rate constants at combustion temperatures and suggests that the dominant product will be IO, with a lesser contribution from OH, and that direct O atom abstraction on the triplet PES will become significant above about 1000 K. Adduct stabilization not only becomes slow, because of the decreasing collisional efficiency of the bath gas as the temperature increases, but also (being exothermic) it becomes thermodynamically unfavorable.

Conclusions

Several transient carbon−oxygen−iodine species have been characterized by ab initio methods. The results are in overall good agreement with the IR spectral assignments where these are available and provide thermochemical data for use in

atmospheric and combustion modeling. Transition states connecting these species have also been characterized and the results used to develop the singlet and triplet potential energy surfaces for the reaction $O + CH_3I$. These surfaces qualitatively explain the complex behavior of this reaction, and a QRRK analysis gave good accord with the recent kinetic and product studies by Gilles et al.[2] This analysis yields insight into the likely high-temperature behavior of this reaction and possible products other than IO and OH. IO is the dominant product predicted below about 2000 K.

Acknowledgment. We thank Drs. M. P. McGrath and L. Radom for valuable advice about their G2 extension and a preprint of ref 7, Drs. M. K. Gilles and A. R. Ravishankara for a preprint of ref 2 and helpful comments, Dr. R. Grice for valuable discussions, and Dr. R. E. Huie for a preprint of ref 11. This work was supported in part by the Air Force Office of Scientific Research and its SFRP and SERP programs, the R. A. Welch Foundation (Grant B-1174), and the UNT Faculty Research Fund. Computational resources were provided by the Wright Laboratory at Wright-Patterson AFB and by Dr. M. Schwartz at UNT.

References and Notes

(1) Tapscott, R. E.; Skaggs, S. R.; Diedorf, D. In *Halon Replacements. Technology and Science*; Miziolek, A. W., Tsang, W., Eds.; ACS Symposium Series 611; American Chemical Society: Washington, DC, 1995; Chapter 14.

(2) Gilles, M. K.; Turnipseed, A. A.; Talukdar, R. K.; Rudich, Y.; Villalta, P. W.; Huey, L. G.; Burkholder, J. B.; Ravishankara, A. R. *J. Phys. Chem.* **1996**, *100*, 14005.

(3) Solomon, S.; Garcia, R. R.; Ravishankara, A. R. *J. Geophys. Res.* **1994**, *99*, 20491.

(4) Barnes, I.; Becker, K. H.; Starcke, J. *Chem. Phys. Lett.* **1995**, *246*, 594.

(5) Hawkins, M.; Andrews, L. *Inorg. Chem.* **1985**, *24*, 3285.

(6) Curtiss, L. A.; Raghavachari, K.; Trucks, G. W.; Pople, J. A. *J. Chem. Phys.* **1991**, *94*, 7221.

(7) Glukhovtsev, M. N.; Pross, A.; McGrath, M. P.; Radom, L. *J. Chem. Phys.* **1995**, *103*, 1878.

(8) Frisch, M. J.; Trucks, G. W.; Schlegel, H. B.; Gill, P. M. W.; Johnson, B. G.; Robb, M. A.; Cheeseman, J. R.; Keith, T.; Petersson, G. A.; Montgomery, J. A.; Raghavachari, K.; Al-Laham, M. A.; Zakrzewski, V. G.; Ortiz, J. V.; Foresman, J. B.; Cioslowski, J.; Stefanov, B. B.; Nanayakkara, A.; Challacombe, M.; Peng, C. Y.; Ayala, P. Y.; Chen, W.; Wong, M. W.; Andres, J. L.; Replogle, E. S.; Gomperts, R.; Martin, R. L.; Fox, D. J.; Binkley, J. S.; DeFrees, D. J.; Baker, J.; Stewart, J. J. P.; Head-Gordon, M.; Gonzalez, C.; Pople, J. A. *GAUSSIAN94*; Gaussian: Pittsburgh, PA, 1995.

(9) Gurvich, L. V.; Veyts, I. V.; Alcock, B. B. *Thermodynamic Properties of Individual Substances*; Hemisphere: New York, 1989.

(10) McGrath, M. P.; Rowland, F. S. *J. Phys. Chem.* **1996**, *100*, 4815.

(11) Huie, R. E.; Laszlo, B. In *Halon Replacements. Technology and Science*; Miziolek, A. W., Tsang, W., Eds.; ACS Symposium Series 611; American Chemical Society: Washington, DC, 1995; Chapter 4.

(12) Radlein, D. S. A. G.; Whitehead, J. C.; Grice, R. *Nature* **1975**, *253*, 37.

(13) Buss, R. J.; Sibener, S. J.; Lee, Y. T. *J. Phys. Chem.* **1983**, *87*, 4840.

(14) Berry, R. J.; Yuan, W.-J.; Misra, A.; Marshall, P. To be submitted.

(15) Hassanzadeh, P.; Irikura, K. K. *J. Phys. Chem. A* **1997**, *101*, 1580.

(16) Bedjanian, Y.; Le Bras, G.; Poulet, G. *J. Phys. Chem.* **1996**, *100*, 15130.

(17) Seetula, J. A.; Gutman, D. *J. Phys. Chem.* **1992**, *96*, 5401.

(18) Chase, M. W., Jr.; Davies, C. A.; Downey, J. R., Jr.; Frurip, D. J.; McDonald, R. A.; Syverud, A. N. *JANAF Thermochemical Tables*, 3rd ed.; *J. Phys. Chem. Ref. Data* **1985**, *14* (Suppl. No. 1).

(19) Wang, J. J.; Smith, D. J.; Grice, R. *J. Phys. Chem.* **1996**, *100*, 6620.

(20) Steckler, R.; Hu, W.-P.; Liu, Y.-P.; Lynch, G. C.; Garrett, B. C.; Isaacson, A. D.; Lu, D.-h.; Melissas, V. S.; Truong, T. N.; Rai, S. N.; Hancock, G. C.; Lauderdale, J. G.; Joseph, T.; Truhlar, D. G. *POLYRATE*, version 6.5; University of Minnesota: Minneapolis, MN, 1995.

(21) Johnston, H. S. *Gas-Phase Reaction Rate Theory*; Ronald: New York, 1966; Chapter 2.

(22) Marshall, P.; Ko, T.; Fontijn, A. *J. Phys. Chem.* **1989**, *93*, 1922.

(23) Chen, J.; Catoire, V.; Niki, H. *Chem. Phys. Lett.* **1995**, *245*, 519.

(24) Orlando, J. J.; Tyndall, G. S.; Wallington, T. J. *J. Phys. Chem.* **1996**, *100*, 7026.

(25) Klaassen, J. J.; Lindner, J.; Leone, S. R. *J. Chem. Phys.* **1996**, *104*, 7403.

(26) Loomis, R. A.; Klaassen, J. J.; Lindner, J.; Christopher, P. G.; Leone, S. R. *J. Chem. Phys.* **1997**, *106*, 3934.

(27) Marshall, P.; Misra, A.; Yuan, W.-J.; Berry, R. J. Presented at the 28th Central Regional ACS Meeting, 1996; paper 91.

(28) (a) Dean, A. M. *J. Phys. Chem.* **1985**, *89*, 4600. (b) Westmoreland, P. R. BI_QRRK program, 1993.

(29) Benson, S. W. *Thermochemical Kinetics*; Wiley: New York, 1976; Chapter 3.

(30) Hirschfelder, J. O.; Curtiss, C. F.; Bird, R. B. *Molecular Theory of Gases and Liquids*; Wiley: New York, 1964; p 1122.